Improved Moment Invariants for Invariant Image Representation

R. Palaniappan[+], P.Raveendran[+] and Sigeru Omatu[*]

[+]Dept. of Electrical
Faculty of Engineering,
University of Malaya,
Kuala Lumpur, 50603, Malaysia.

[*]Dept. of Computer and System Science
College of Engineering
University of Osaka Perfecture,
Sakai, Osaka, 593, Japan.

Abstract

This paper proposes improved moment invariants for representing images. These features are invariant to orientation, size and translation. These new features compute moments from a point shifted to a distance from the image centroid. By doing so, the new moments show improved ability to represent symmetrical and noisy images. Both these problems of symmetry and noise are common when regular moment invariants are used. The new reference centre is selected such that the invariant properties like translation, scaling and rotation are maintained. In this paper, we show that these new proposed moments solve the symmetrical problem and are more robust to noise corruption as compared to two different types of regular moment functions derived by Hu [9]. Extensive experimental study using a neural network classification scheme with these moments as inputs are conducted to verify the proposed method.

Keywords: regular moment functions, Hu moment invariants, symmetrical images, noise, neural network.

1.0 Introduction

Moment functions have a broad spectrum of applications in image analysis, such as invariant pattern recognition, object classification, pose estimation, image coding and reconstruction [12]. A set of moments generally represents global characteristics of the image shape and provides information about different types of geometrical features of the image. Regular moments are the first of these moment functions to find applications since they are algorithmically and computationally simple.

One of the earliest significant paper on the application of moments was published by Hu [9] in 1962. His classic paper on pattern recognition has been cited in almost all moment related publications and has received wide attention during the past few decades. His approach was based on the work of the nineteenth century mathematicians Boole, Cayley and Sylvester, on the theory of algebraic forms [6]. He used regular moments to develop a set of non-linear functions called moment-invariants that are invariant to translation, size and rotation, which he applied to a simple character recognition problem. He used central moments and mass normalisation technique to obtain invariance to translation and scaling. He also proposed two different methods for obtaining invariance to rotation. The first method is based on combinations of regular moments using algebraic invariants, which he called as the absolute moment invariants. The other method was derived using the principal axis method. In this paper, we shall refer to both these methods collectively as Hu's moments.

Subsequently, this method was used for pattern recognition by Alt [1] in 1962, ship identification by Smith and Wright [24] in 1971, aircraft identification by Dudani et al. [5] in 1977, pattern matching by Dirilten [4] in 1977 and scene matching by Wong and Hall [24] in 1978.

But there is a problem with using these moments for images with symmetry. Some examples of images with symmetry are like alphanumeric characters and common objects like vehicles (ships, airplanes, cars, buses), furniture (sofa, cupboard), buildings, etc. Images with symmetry in the x and/or y directions and symmetry at centroid give zero values for odd orders of central moments. This is due to the symmetrical location of the image pixels around the centroid, which results in a net central moment calculation of zero. Hu [9] used these central moments to achieve translation invariance and as such, the number of features that are available to represent a symmetrical image is reduced causing poor recognition performance. In computing the seven features of the second and third order invariant moments using the equations shown in [9] for images with symmetry in both x and y directions, only two of the second order moments produce nonzero values. The problem becomes worse under noisy environments where more features are required for successful recognition since most classifiers are trained only with noiseless images.

Regular moment functions are also highly sensitive to noise and this problem has been the topic of interest for many researchers [7],[10],[23]. This sensitivity is caused by the moments' dependence on the powers of the x-distance and y-distance of each pixel from the centroid (or centre of the co-ordinate system) and since the image pixels are generally located closer to the centroid than the noise speckles, it is evident that the presence of a few noise grains would profoundly affect the values of the moments thus resulting in almost impossible recognition. Although adopting lower order moments will reduce the severity of the problem, the higher order moments represent the finer details of the image and as such are necessary for successful recognition especially under low interclass variance problems.

In this paper, both these problems are addressed and a single solution is proposed to solve them. The solution involves in obtaining a set of new moment features, which are computed from a reference centre shifted further away from the centroid of the image. This new centre is selected in such a way that the new moments are invariant to properties like translation, scale and rotation. This technique produces nonzero values for all the features of any order and thereby solving the problem caused by symmetrical images for regular moment functions. Due to the fact that the new centre is shifted further away from the image centroid, all the pixels contribute a higher value to moment calculation. Since most noisy images have much higher signal content than noise content, the contribution of the signal pixels is greatly increased as compared to contribution of noise pixels which only increases slightly. As such, the new moments are more tolerant to noise corruption.

In Section II, we describe the basic theory of regular moments along with a description on the symmetrical problem. Section III deals with the derivation of the new moment equations and proves the scale and translation invariant properties. The next portion of this section shows that the new moments can solve the symmetrical problem. Section IV deals with invariance of rotated images using the new moments. The next section treats the application of the new moments for images corrupted with noise and shows the improvement of noise tolerance of the new moments as compared to both of Hu's moments. Section VI treats the extensive computer simulations of Neural Network (NN) classification using symmetrical and non-symmetrical images corrupted with Gaussian and random probability noise. Section VII provides the conclusion.

2.0 Basic Theory of Regular Moments and Symmetrical Problem

The regular moments are defined as:

$$m_{pq} = \int_{-\infty}^{\infty} \int_{-\infty}^{\infty} x^p y^q f(x, y) dx dy \tag{1}$$

with $p,q \in N_0$ as order indices, (x,y) are Cartesian coordinates; f is a non-negative continuos image function with bounded support so that integration within the available image plane is sufficient to

gather all the signal information. In this paper, only binary image functions are considered so *f(x,y)* can only be 0 or 1.

For digital images with an *M x M* array of pixels, the double integration in (1) is approximated by summation formulas. The regular moments are then computed from

$$m_{pq} = \sum_{0}^{M-1}\sum_{0}^{M-1} x^p y^q f(x,y) \tag{2}$$

To keep the dynamic range of m_{pq} consistent for different images, the *M x M* image plane is limited to the square satisfying the condition |x|, |y| ≤ 1. This implies that the grid locations will no longer be integers but will have real values in the [-1,+1] range. This changes the definition of m_{pq} to

$$m_{pq} = \sum_{-1}^{+1}\sum_{-1}^{+1} x^p y^q f(x,y) \tag{3}$$

These moments are made invariant to translation and scaling by using the following invariant [9]:

$$\eta_{pq} = \frac{\mu_{pq}}{m_{00}^{\frac{(p+q+2)}{2}}} \tag{4}$$

where the central moments, μ_{pq} are defined as

$$\mu_{pq} = \sum_{-1}^{+1}\sum_{-1}^{+1} \left(x-\bar{x}\right)^p \left(y-\bar{y}\right)^q \mathrm{f(x,y)} \tag{5}$$

with $\bar{x}$ and $\bar{y}$ as the coordinates of the image centroid given by

$$\bar{x} = \frac{m_{10}}{m_{00}}, \qquad \bar{y} = \frac{m_{01}}{m_{00}} \tag{6}$$

For binary images, m_{00} represents the total number of pixels in the image.

Now consider Figure 1 as an illustration to describe the symmetrical problem faced by central moments. This figure depicts an image that is symmetrical in both x and y axes. For the image shown in Figure 1, if *p* and/or *q* take an odd number then μ_{pq} becomes zero.

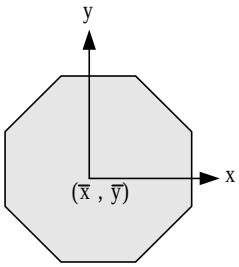

Figure 1: A symmetrical image

Table 1 gives regular moment functions for various scaled and translated symmetrical images and it can be seen that many moments are zero for these type of images.

Table 1: Regular moment invariants for various translated and scaled symmetrical images

Image	Symmetry Type	Scaling factors	η_{02}	η_{20}	η_{11}	η_{12}	η_{21}	η_{03}	η_{30}
O	Symmetry at both x & y axis	a=1.0	1.73e-1	1.89e-1	0.0	0.0	0.0	0.0	0.0
O		a=2.0	1.73e-1	1.89e-1	0.0	0.0	0.0	0.0	0.0
D	Symmetry at x axis	a=1.0	1.41e-1	1.96e-1	0.0	0.0	9.02e-3	8.69e-3	0.0
D		a=2.0	1.41e-1	1.96e-1	0.0	0.0	9.02e-3	8.69e-3	0.0
U	Symmetry at y axis	a=1.0	1.75e-1	2.01e-1	0.0	2.08e-2	0.0	0.0	1.26e-2
U		a=2.0	1.75e-1	2.01e-1	0.0	2.08e-2	0.0	0.0	1.26e-2
Z	Symmetry at centroid	a=1.0	9.30e-2	2.83e-1	6.25e-2	0.0	0.0	0.0	0.0
Z		a=2.0	9.30e-2	2.83e-1	6.25e-2	0.0	0.0	0.0	0.0

Now, if we were to shift the reference centre (i.e. the co-ordinate system) further away from the centroid of the image then μ_{pq} becomes nonzero even though p and/or q takes an odd number. But the new centre has to be chosen such that all the invariance properties are still maintained. In the following section, we develop the theory and the equations used in deriving the new moments using a shifted reference centre.

3.0 New Moments

Let us define the new central moments as

$$\lambda_{pq} = \int_{-\infty}^{\infty}\int_{-\infty}^{\infty} \left(x - \bar{x} + x_s\right)^p \left(y - \bar{y} + y_s\right)^q f(x,y)dxdy \tag{7}$$

where the shift factors; x_s and y_s are defined as

$$x_s = \left(\frac{\mu_{20}}{m_{00}}\right)^{1/2} \text{ and } y_s = \left(\frac{\mu_{02}}{m_{00}}\right)^{1/2} \tag{8}$$

For digital images as considered in this paper, the new central moments are defined as

$$\lambda_{pq} = \sum_{-1}^{+1}\sum_{-1}^{+1} \left(x - \bar{x} + x_s\right)^p \left(y - \bar{y} + y_s\right)^q f(x,y) \tag{9}$$

To determine the shift-invariance of λ_{pq}, let the image function

$$g(x,y) = f(x-x_0, y-y_0) \tag{10}$$

be a shifted version of the given image function, *f(x,y)*. Substituting (10) in (7), it is seen that λ_{pq} is the same for *f(x,y)* and *g(x,y)* and hence it is invariant to translation.

The new central moments can be normalised to become invariant to scale change by defining,

$$\phi_{pq} = \frac{\lambda_{pq}}{m_{00}^{(p+q+2)/2}} \tag{11}$$

To show the scale invariance of the new moments, let

$$h(x, y) = f(\frac{x}{a}, \frac{y}{a}) \tag{12}$$

represent a scaled version of the given image function, *f(x,y)*. Then the new central moments, $\tilde{\lambda}_{pq}$ evaluated for the scaled image, *h(x,y)* is

$$\begin{aligned}\tilde{\lambda}_{pq} &= \int_{-\infty}^{\infty}\int_{-\infty}^{\infty} (x - \bar{x} + x_s)^p (y - \bar{y} + y_s)^q f(\frac{x}{a}, \frac{y}{a}) dxdy \\ &= \int_{-\infty}^{\infty}\int_{-\infty}^{\infty} (ax - a\bar{x} + ax_s)^p (by - b\bar{y} + by_s)^q abf(x, y) dxdy \\ &= a^{p+q+2}\lambda_{pq}\end{aligned} \tag{13}$$

Combining (11) and (13), it is evident that $\tilde{\phi}_{pq}$, for the scaled image is the same as for the original image, ϕ_{pq} thus giving us moments which are invariant to scaling.

The values in Table 2 prove that these new moments are invariant to scaling and translation and it also shows that these new moments do not give any zero values for various types of symmetrical images thereby solving the symmetrical image problem faced by central moments.

4.0 New Moments for Rotated Images

In this paper, two techniques are proposed to obtain invariance to rotation for the new moments. The first method involves unrotating the image using the principal axis method [9] and moments in the principal axis can be obtained which are invariant to rotation. This is performed by computing the second order central moments using (5) and obtaining the angle, θ that the image has rotated from the principal axis with the equation given below [9]:

$$\theta = \frac{1}{2}\tan^{-1}\frac{2u_{11}}{u_{20} - u_{02}} \tag{14}$$

Next the image is unrotated to its principal axis and the new moments are calculated using (7) for continuous images or (9) for digital images. But this method is erroneous for digital images since there would be some pixels lost while performing the unrotation of the image.

Table 2: New moments as proposed in this paper for various translated and scaled symmetrical images

Image	Symmetry Type	Scaling factors	ϕ_{02}	ϕ_{20}	ϕ_{11}	ϕ_{12}	ϕ_{21}	ϕ_{03}	ϕ_{30}
O	Symmetry at both x & y axis	a=1.0	3.45e-1	3.78e-1	1.81e-1	7.65e-3	7.97e-3	2.20e-2	2.56e-2
O		a=2.0	3.45e-1	3.78e-1	1.81e-1	7.65e-3	7.97e-3	2.20e-2	2.56e-2
D	Symmetry at x axis	a=1.0	2.86e-1	3.91e-1	1.67e-1	6.45e-3	1.65e-2	2.49e-2	2.67e-2
D		a=2.0	2.86e-1	3.91e-1	1.67e-1	6.45e-3	1.65e-2	2.49e-2	2.67e-2
U	Symmetry at y axis	a=1.0	3.51e-1	4.02e-1	1.88e-1	2.87e-2	8.58e-3	2.25e-2	3.97e-2
U		a=2.0	3.51e-1	4.02e-1	1.88e-1	2.87e-2	8.58e-3	2.25e-2	3.97e-2
Z	Symmetry at centroid	a=1.0	1.86e-1	5.66e-1	1.62e-1	1.12e-2	8.92e-3	1.27e-2	5.49e-2
Z		a=2.0	1.86e-1	5.66e-1	1.62e-1	1.12e-2	8.92e-3	1.27e-2	5.49e-2

To overcome this limitation of the first method, we are proposing another technique to obtain invariance to rotation for the new moments. In the second technique, we use the relationship between regular moments and rotation to obtain μ_{pq}^{ur} which are the regular central moment defined in the principal axis [12]. To explain further, let us express the central moments from (5) in polar form and for simplicity, we assume that the co-ordinate origin has been chosen to coincide with the image centroid. These moments, μ_{pq} in polar form are

$$\mu_{pq} = \sum_{\zeta}\sum_{\zeta}(r\cos\chi)^p(r\sin\chi)^q rf(r,\chi) \quad \text{for p,q = 0,1,2,.....} \tag{15}$$

where $x = r\cos\chi$ and $y = r\sin\chi$ and the Jacobian of the transformation is r while ζ denotes the normalised image region of the x-y plane defined in (5).

Now, consider the fact that the image has rotated through an angle θ. By a change of variable $\varphi = \chi - \theta$, the central moments for the rotated image, μ_{pq}^{r}, are

$$\mu^{r}{}_{pq} = \sum_{\zeta}\sum_{\zeta}(r\cos(\theta+\varphi))^p(r\sin(\theta+\varphi))^q rf(r,\varphi) \tag{16}$$

As can be seen from (16), the angle of rotation is used in computing the moments when an image is rotated. So moments for rotated image can be computed easily if the angle of rotation is known.

Similarly, a relationship between the original central moments, μ_{pq} and the rotated central moments, μ^{r}_{pq} can be established by expanding (16) and expressing it in terms of the moments of the original image. If the image rotates through an angle θ, the moments change according to [12]

$$\mu^{\mathrm{r}}\mathrm{pq} = \sum_{r=0}^{p}\sum_{s=0}^{q}(-1)^{q-s}\binom{p}{r}\binom{q}{s}(\cos\theta)^{p-r+s}(\sin\theta)^{q+r-s}(\mu_{\mathrm{p+q-r-s,r+s}}) \tag{17}$$

Using a similar analysis, we are able to get the unrotated central moment, μ^{ur}_{pq} which are invariant to rotation and translation. These moments are given by the equation below [12]:

$$\mu^{ur}_{pq} = \sum_{r=0}^{p}\sum_{s=0}^{q}(-1)^{p+q-r}\binom{p}{r}\binom{q}{s}(\cos\theta)^{p-r+s}(\sin\theta)^{q+r-s}\mu_{(p+q-r-s,r+s)} \tag{18}$$

where the angle, θ is obtained from (14) and μ_{pq} is calculated from (5).

By expanding (7) or (9), a relationship between the regular central moments and the new central moments can be established. The general form of the derived relationship for the digital images used in this paper is as given below:

$$\lambda_{pq} = \sum_{-1}^{+1}\sum_{-1}^{+1}\Big[\sum_{i=0}^{p}\binom{p}{i}(x-\bar{x})^{p-i}x_s^{i}\sum_{j=0}^{q}\binom{q}{j}(y-\bar{y})^{q-j}y_s^{j}\Big] \tag{19}$$

Combining this relationship with the unrotated regular central moments, μ^{ur}_{pq} obtained from (18), the new central moments invariant to rotation, λ^{ur}_{pq} can be derived. The equations for the new central moments using this method up to the third order moments are as listed below:

$$\begin{aligned}
\lambda^{ur}_{20} &= \mu^{ur}_{20} + m_{00}x_s^2\\
\lambda^{ur}_{02} &= \mu^{ur}_{02} + m_{00}y_s^2\\
\lambda^{ur}_{11} &= \mu^{ur}_{11} + m_{00}x_s y_s\\
\lambda^{ur}_{30} &= \mu^{ur}_{30} + 3\mu^{ur}_{20}x_s + m_{00}x_s^3\\
\lambda^{ur}_{03} &= \mu^{ur}_{03} + 3\mu^{ur}_{02}y_s + m_{00}y_s^3\\
\lambda^{ur}_{21} &= \mu^{ur}_{21} + \mu^{ur}_{20}y_s + 2\mu^{ur}{}_{11}x_s + m_{00}x_s^2y_s\\
\lambda^{ur}_{12} &= \mu^{ur}_{12} + \mu^{ur}_{02}x_s + 2\mu^{ur}{}_{11}y_s + m_{00}x_s y_s^2
\end{aligned} \tag{20}$$

where the shift factors x_s and y_s are obtained from (8).

There are two advantages of using the latter technique as compared to the earlier. First, it will produce the new moments without any error surfacing from the process of unrotating the image for digital images. Secondly, this method is computationally much faster as compared to the earlier method since it involves only addition operators as can be seen from (20). The moments λ^{ur}_{pq} are inserted into (11) to obtain ϕ_{pq} which are invariant to translation, scaling and rotation.

Table 3 shows the values of the new moments for different types of rotated symmetrical images with a 60° angle of rotation. From this table, it can be seen that the new moments are invariant to rotation. Exact values are not obtained within a class since the images are digital.

Table 3: New moments as proposed in this paper for various types of rotated symmetrical images with a 60° angle of rotation

Image	Symmetry Type	ϕ_{02}	ϕ_{20}	ϕ_{11}	ϕ_{12}	ϕ_{21}	ϕ_{03}	ϕ_{30}
	Symmetry at both x & y axis	3.45e-1	3.78e-1	1.81e-1	7.65e-3	7.97e-3	2.20e-2	2.56e-2
		3.46e-1	3.79e-1	1.81e-1	7.68e-3	7.92e-3	2.19e-2	2.58e-2
	Symmetry at x axis	2.86e-1	3.91e-1	1.67e-1	6.45e-3	1.65e-2	2.49e-2	2.67e-2
		2.87e-1	3.92e-1	1.68e-1	6.56e-3	1.65e-2	2.50e-2	2.67e-2
	Symmetry at y axis	3.51e-1	4.02e-1	1.88e-1	2.87e-2	8.58e-3	2.25e-2	3.97e-2
		3.51e-1	4.03e-1	1.88e-1	2.87e-2	8.52e-3	2.37e-2	3.97e-2
	Symmetry at centroid	1.86e-1	5.66e-1	1.62e-1	1.12e-2	8.92e-3	1.27e-2	5.49e-2
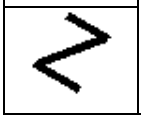		1.86e-1	5.66e-1	1.62e-1	1.13e-2	8.81e-3	1.27e-2	5.48e-2

5.0 New Moments for Noisy Images

Figure 2 shows two different classes of images corrupted with different random noise levels. The noise percentage is calculated based on the image capture area, i.e. the 128 x 128 resolution grid. As an example, 0.5% noise would signify that 81 pixels of noise have been added to the image. Since binary images are considered in this paper, this means that the values of 81 pixels in the image are changed from 0 to 1 or vice versa.

Tables 4 (a) and (b) give the values of both types of Hu's moments and the new moments for these images. The sample mean is denoted by μ, the sample deviation by σ and the percentage spread of moments from their corresponding mean by $\sigma/\mu\%$. From the values of $\sigma/\mu\%$, it can be seen that both type of Hu's moments are very sensitive to noise especially the higher order moments. Hu's absolute moment invariants are much more perturbed by noise as compared to Hu's principal axis moments since the earlier involves combination of many moments with their noise errors added whereas for the latter case, only the individual moment noise error surfaces. It can also be seen that η_{11} from Hu's principal axis moment is zero for all the images since μ_{11} equal to zero is the condition necessary to obtain the principal axis.

Random Noise Level					
0%	0.1%	0.2%	0.3%	0.4%	0.5%
					
					

Figure 2: Examples of two different images with different levels of random noise added

Comparing the average sum of σ/μ% in Table 4 (a) and (b), we can deduce that the new moments are less sensitive under noisy environments as compared to both types of Hu's moments. This is due to the fact that the new moments uses a reference centre shifted further away from the image centroid and as a result, the contribution of the signal pixels is greatly increased as compared to the contribution of noise pixels which only increases slightly. This is since for most images corrupted with noise, the signal content is much higher than the noise content. As such, the new moments are much less perturbed by the noise pixels and this is also the reason why the new moments are better invariant features than both types of Hu's moments for rotated digital images due to loss of signal pixels while performing rotation. The value of σ/μ% for ϕ_{20} and ϕ_{02} are the same as for η_{20} and η_{02}, respectively since the shift factors x_s and y_s are in terms of μ_{20} and μ_{02}. Therefore, the percentage errors due to noise for both cases do not change. But the other values of σ/μ% for the new moments are significantly lower than both types of Hu's moments which indicates the higher noise tolerance of the new moments.

6.0 Experimental Study

All the images for this study are drawn on a 128-resolution image plane and the image plane is mapped onto a square defined by $x \in [-1,+1]$, $y \in [-1,+1]$ before performing any moment calculations. Two different data sets of 26 classes, i.e. alphabets from A to Z are used in the experiments. The first set consists of the Arial font where most of the 26 characters of this font have at least one of the symmetrical property listed in column two of Tables 1 and 2. Figure 3 shows the base set (i.e. without any scaling and rotation) of the alphabets from the Arial font selected for the first experimental study. The second data set consists of the Times New Roman font. Figure 4 shows the base set of the alphabets from this font. This particular font is chosen since many word processor users use it frequently and also since it consists mostly of non-symmetrical characters. The data set for each class consists of 13 different scale factors and rotation angles (inclusive of the base image) as shown in Figure 5 for an image A.

In this paper, a comparison on the effects of Gaussian and random noise distribution for NN classification using both the Hu's moments and the new moments are studied. The probability (normalised to unity) of a Gaussian noise pixel occuring at *(x,y)* is given by

$$p(x,y) = \frac{1}{2\pi\sigma_x\sigma_y}\exp\left[-\left(\frac{(x-x_0)^2}{2\sigma_x} + \frac{(y-y_0)^2}{2\sigma_y}\right)\right] \tag{21}$$

where x_0 and y_0 represent the mean of x and y values , σ_x^2 and σ_y^2 represent the x variance and y variance, respectively. A random function generator is used to obtain the random noise.

A	B	C	D	E	F	G	H	I
J	K	L	M	N	O	P	Q	R
S	T	U	V	W	X	Y	Z	

Figure 3: Alphabets from Arial font used for symmetrical data simulation

Table 4 (a): Results of different moments for random type noisy image J shown in Figure 2

Noise		No noise	0.1% random noise	0.2% random noise	0.3% random noise	0.4% random noise	0.5% random noise	μ	σ	σ/μ %
Image										
Hu's moments using principal axis method	η_{02}	6.72e-2	7.23e-2	7.86e-2	8.87e-2	9.22e-2	1.07e-1	8.43e-2	1.44e-2	17.141
	η_{20}	3.46e-1	3.50e-1	3.51e-1	3.52e-1	3.56e-1	3.56e-1	3.52e-1	3.83e-3	1.087
	η_{11}	0.0	0.0	0.0	0.0	0.0	0.0	0.0	0.0	0.0
	η_{12}	1.65e-2	1.55e-2	1.67e-2	1.84e-2	1.87e-2	7.50e-3	1.55e-2	4.12e-3	26.481
	η_{21}	3.56e-2	3.33e-2	3.55e-2	3.71e-2	3.74e-2	3.19e-2	3.51e-2	2.13e-3	6.070
	η_{03}	4.93e-3	2.48e-3	1.65e-2	1.67e-2	1.92e-2	3.36e-2	1.56e-2	1.12e-2	71.844
	η_{30}	7.05e-2	6.87e-2	7.17e-2	6.77e-2	6.66e-2	6.79e-2	6.88e-2	1.89e-3	2.744
Average of sum for σ/μ%										**20.894**
Hu's absolute moment invariants	m_1	4.14e-1	4.22e-1	4.29e-1	4.41e-1	4.49e-1	4.63e-1	4.36e-1	1.80e-2	4.127
	m_2	7.80e-2	7.71e-2	7.42e-2	6.93e-2	6.99e-2	6.23e-2	7.18e-2	5.86e-3	8.165
	m_3	2.47e-2	2.28e-2	2.29e-2	2.40e-2	2.37e-2	1.20e-2	2.17e-2	4.78e-3	22.042
	m_4	4.56e-3	4.11e-3	5.73e-3	5.32e-3	5.50e-3	7.94e-3	5.53e-3	1.33e-3	24.131
	m_5	1.63e-5	1.88e-5	4.21e-6	1.54e-5	2.35e-5	2.33e-5	1.69e-5	7.09e-6	41.926
	m_6	3.57e-4	4.28e-4	8.80e-5	1.20e-4	2.38e-4	1.61e-4	2.32e-4	1.36e-4	58.561
	m_7	4.55e-5	3.50e-5	6.55e-5	5.82e-5	5.82e-5	7.42e-5	5.61e-5	1.40e-5	24.981
Average of sum for σ/μ%										**26.276**
New moments	ϕ_{02}	1.34e-1	1.45e-1	1.57e-1	1.77e-1	1.84e-1	2.13e-1	1.69e-1	2.89e-2	17.141
	ϕ_{20}	6.93e-1	7.00e-1	7.02e-1	7.04e-1	7.13e-1	7.12e-1	7.04e-1	7.65e-3	1.087
	ϕ_{11}	1.53e-1	1.59e-1	1.66e-1	1.77e-1	1.81e-1	1.95e-1	1.72e-1	1.55e-2	9.035
	ϕ_{12}	2.05e-2	1.99e-2	2.14e-2	2.37e-2	2.42e-2	2.39e-2	2.23e-2	1.93e-3	8.652
	ϕ_{21}	4.46e-2	4.28e-2	4.54e-2	4.77e-2	4.83e-2	4.37e-2	4.54e-2	2.19e-3	4.810
	ϕ_{03}	2.02e-2	2.34e-2	2.31e-2	2.46e-2	2.76e-2	2.44e-2	2.39e-2	2.41e-3	10.094
	ϕ_{30}	1.32e-1	1.31e-1	1.34e-1	1.31e-1	1.31e-1	1.32e-1	1.32e-1	1.37e-3	1.040
Average of sum for σ/μ%										**7.408**

Each image is subjected to 5 levels of Gaussian and random noise corruption from 0.1% to 0.5% in steps of 0.1. Therefore, the Arial data set of 26 classes consists of 338 noiseless images, 1690 images with random noise and 1690 images with Gaussian noise. The Times New Roman data set also consists of a similar amount of images.

In this experiment, NN topology known as multilayer perceptron (MLP) with one hidden layer is used to classify the 26 class problem of two different sets of images, one symmetrical and the other non-symmetrical English alphabets explained previously. Figure 6 shows a diagram of MLP with one hidden layer. The back-propagation algorithm [20] is used to train the NN.

Five different numbers of hidden units of 10, 15, 20, 25 and 30 are used for all the experiments. The NN is trained with only the base 26 noiseless alphabets for both the symmetrical and the non-symmetrical cases. The training error limit is set at 0.001 for all experiments. The test is conducted

with the 338 images from the 13 different scale factors and rotation angles for both the noise and noiseless cases. The inputs to the NN consist of 7 moment features for all the experiments except for the case of Hu's principal axis moments which has only 6 moment features since μ_{11} is zero for all the images in this method. The output is fixed to 26 classes for all the experiments.

Since the numerical values of m_1 to m_7 (Hu's absolute moment invariants) are very small, the logarithms of the absolute values of these functions are used. To ensure equal conditions for all the experiments, logarithms of the absolute values are also used for Hu's principal axis moments and the new moments proposed in this paper. All the inputs to the NN are normalised from 0 to 1 to avoid the NN weights from becoming unstable during training.

For the ease of reference, the moment equations used by Hu [9] are briefly explained here. Hu's principal axis moment invariants are obtained by inserting μ_{pq}^{ur} from (18) into (4) to obtain η_{pq}. A disadvantage of this method is that it would only have 6 moment features up to the third order since it requires μ_{11} to be zero to achieve invariance to rotation. Hu's absolute moment invariants up to the third order are as given below:

$$
\begin{aligned}
m_1 &= \eta_{20} + \eta_{02} \\
m_2 &= (\eta_{20} - \eta_{02})^2 + 4\eta_{11} \\
m_3 &= (\eta_{30} - 3\eta_{12})^2 + (3\eta_{21} - \eta_{03})^2 \\
m_4 &= (\eta_{30} + \eta_{12})^2 + (\eta_{21} + \eta_{03})^2 \\
m_5 &= (\eta_{30} - 3\eta_{12})(\eta_{30} + \eta_{12})[(\eta_{30} + \eta_{12})^2 - 3(\eta_{21} + \eta_{03})^2] + \\
&\quad (3\eta_{21} - \eta_{03})(\eta_{21} + \eta_{03})[3(\eta_{30} + \eta_{12})^2 - (\eta_{21} + \eta_{03})^2] \\
m_6 &= (\eta_{20} - \eta_{02})[(\eta_{30} + \eta_{12})^2 - (\eta_{21} + \eta_{03})^2] + 4\eta_{11}(\eta_{30} + \eta_{12})(\eta_{21} + \eta_{03}) \\
m_7 &= (3\eta_{21} - \eta_{03})(\eta_{30} + \eta_{12})[(\eta_{30} + \eta_{12})^2 - 3(\eta_{21} + \eta_{03})^2] + \\
&\quad (\eta_{30} + \eta_{12})(\eta_{21} + \eta_{03})[3(\eta_{30} + \eta_{12})^2 - (\eta_{21} + \eta_{03})^2]
\end{aligned}
\tag{22}
$$

The NN classification results for random and Gaussian type noisy images using both the Hu's moments and the new moments for the Arial font are listed in Figure 7. The results clearly indicate that the new moments outperform both of Hu's moments for all the tested noise levels. The results from the noiseless testing shows that the new moments are also less susceptible to digitisation errors caused by rotation of digital images.

A	**B**	**C**	**D**	**E**	**F**	**G**	**H**	**I**
J	**K**	**L**	**M**	**N**	**O**	**P**	**Q**	**R**
S	**T**	**U**	**V**	**W**	**X**	**Y**	**Z**	

Figure 4: Times New Roman alphabets used for non-symmetrical data simulation

Figure 8 shows the NN classification results of using both the Hu's moments and the new moments for the Times New Roman font with Gaussian and random type noisy images. The results again confirm the fact that the new moments outperform both of Hu's moments. The new moments are also less susceptible to digitisation errors caused by rotation of digital images as can be seen from the noiseless testing results.

Image	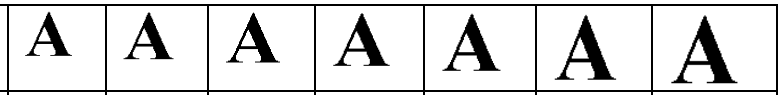						
Scale factor	0.7	0.8	0.9	1.0	1.1	1.2	1.3

(a)

Image	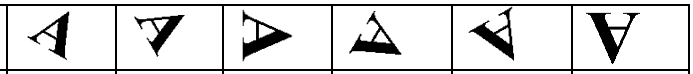					
Angle	30°	60°	90°	120°	150°	180°

(b)

Figure 5: Example of an image A (a) with 13 different scale factors (b) with 6 rotation angles used in the experimental data set

Table 4 (b): Results of different moments for random type noisy image L shown in Figure 2

Noise		No noise	0.1% random noise	0.2% random noise	0.3% random noise	0.4% random noise	0.5% random noise	μ	σ	σ/μ %
Image										
Hu's moments using principal axis method	η_{02}	7.69e-2	8.57e-2	8.66e-2	9.44e-2	9.91e-2	1.08e-1	9.17e-2	1.09e-2	11.881
	η_{20}	3.75e-1	3.77e-1	3.78e-1	3.79e-1	3.80e-1	3.86e-1	3.79e-1	3.66e-3	0.965
	η_{11}	0.0	0.0	0.0	0.0	0.0	0.0	0.0	0.0	0.0
	η_{12}	2.54e-2	2.56e-2	2.14e-2	2.33e-2	2.25e-2	2.00e-2	2.30e-2	2.23e-3	9.686
	η_{21}	5.95e-2	5.87e-2	5.89e-2	6.12e-2	5.97e-2	5.60e-2	5.90e-2	1.71e-3	2.896
	η_{03}	4.28e-3	1.58e-2	8.55e-3	9.84e-3	1.22e-2	2.95e-2	1.34e-2	8.79e-3	65.738
	η_{30}	6.56e-2	6.20e-2	6.58e-2	6.05e-2	6.10e-2	6.28e-2	6.30e-2	2.29e-3	3.633
Average of sum for σ/μ%										**15.800**
Hu's absolute moment invariants	m_1	4.52e-1	4.63e-1	4.65e-1	4.74e-1	4.79e-1	4.94e-1	4.71e-1	1.44e-2	3.049
	m_2	8.91e-2	8.48e-2	8.50e-2	8.11e-2	7.86e-2	7.76e-2	8.27e-2	4.39e-3	5.308
	m_3	5.05e-2	4.50e-2	4.52e-2	4.72e-2	4.44e-2	3.43e-2	4.44e-2	5.46e-3	12.284
	m_4	5.69e-3	6.87e-3	6.53e-3	6.44e-3	6.65e-3	9.16e-3	6.89e-3	1.18e-3	17.147
	m_5	5.19e-5	9.62e-5	5.20e-5	7.78e-5	7.85e-5	1.27e-4	8.06e-5	2.85e-5	35.413
	m_6	7.34e-4	1.23e-3	7.53e-4	1.04e-3	1.04e-3	1.53e-3	1.05e-3	2.99e-4	28.373
	m_7	8.13e-5	7.31e-5	9.94e-5	8.09e-5	8.32e-5	1.01e-4	8.64e-5	1.11e-5	12.825
Average of sum for σ/μ%										**16.343**
New moments	ϕ_{02}	1.54e-1	1.71e-1	1.73e-1	1.89e-1	1.98e-1	2.15e-1	1.83e-1	2.18e-2	11.881
	ϕ_{20}	7.51e-1	7.54e-1	7.56e-1	7.58e-1	7.59e-1	7.72e-1	7.58e-1	7.32e-3	0.965
	ϕ_{11}	1.70e-1	1.80e-1	1.81e-1	1.89e-1	1.94e-1	2.04e-1	1.86e-1	1.19e-2	6.402
	ϕ_{12}	3.02e-2	3.09e-2	2.68e-2	2.91e-2	2.87e-2	2.67e-2	2.87e-2	1.74e-3	6.051
	ϕ_{21}	7.01e-2	6.99e-2	7.02e-2	7.30e-2	7.18e-2	6.88e-2	7.06e-2	1.51e-3	2.133
	ϕ_{03}	1.67e-2	2.03e-2	1.62e-2	1.86e-2	2.16e-2	2.01e-2	1.89e-2	2.16e-3	11.387
	ϕ_{30}	1.35e-1	1.32e-1	1.36e-1	1.31e-1	1.31e-1	1.35e-1	1.33e-1	2.21e-3	1.658
Average of sum for σ/μ%										**5.783**

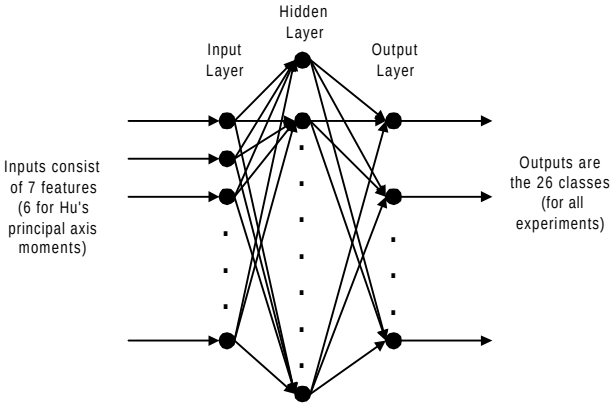

Figure 6: MLP neural network used in the experimental study

7.0 Conclusion

Odd orders of central moments gives zero value for images with symmetry in the x and/or y directions and symmetry at centroid. Regular moment functions are also very sensitive to noise especially the higher order moments. This paper proposes new moment invariants that solves the symmetrical problem faced with regular moment functions and in addition, it is also shown that these new moments are less sensitive to noise and digitisation error than both of the regular moment functions derived by Hu [9].

The solution involves in obtaining a set of new moment features, which are computed from a reference centre shifted further away from the centroid of the image. This new centre is selected in such a way that the new moments are invariant to properties such as translation, scale and rotation. This technique produces nonzero values for all the features of any order and thereby solving the problem caused by symmetrical images for regular moment functions. Since the new centre is shifted further away from the image centroid, the contribution of both the signal and noise pixels are increased but the contribution of signal pixels is much higher than noise pixels. This is due to the fact that most noisy images have a higher signal content than noise content. As such, the new moments are much less perturbed by the noise pixels.

This is also the reason why the new moments are better invariant features than Hu's moments for rotated digital images since some signal pixels are lost while performing rotation. Extensive results of neural network classification for symmetrical and non-symmetrical images using noiseless and two types of random and Gaussian probability noise are presented to validate the proposed method.

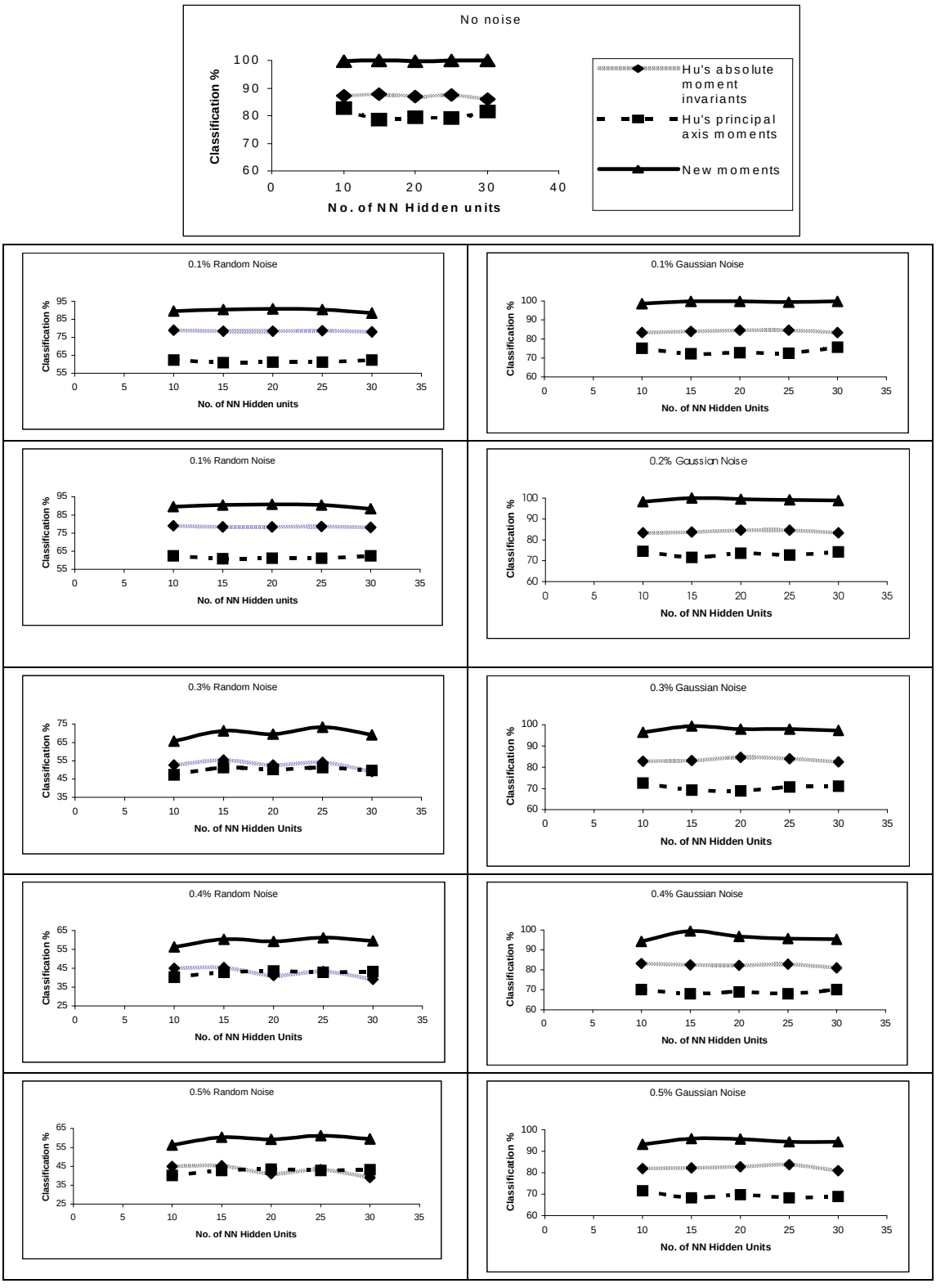

Figure 7: Results of NN classification for Gaussian and random type noisy images from the Arial font for both the Hu's moments and the new moments

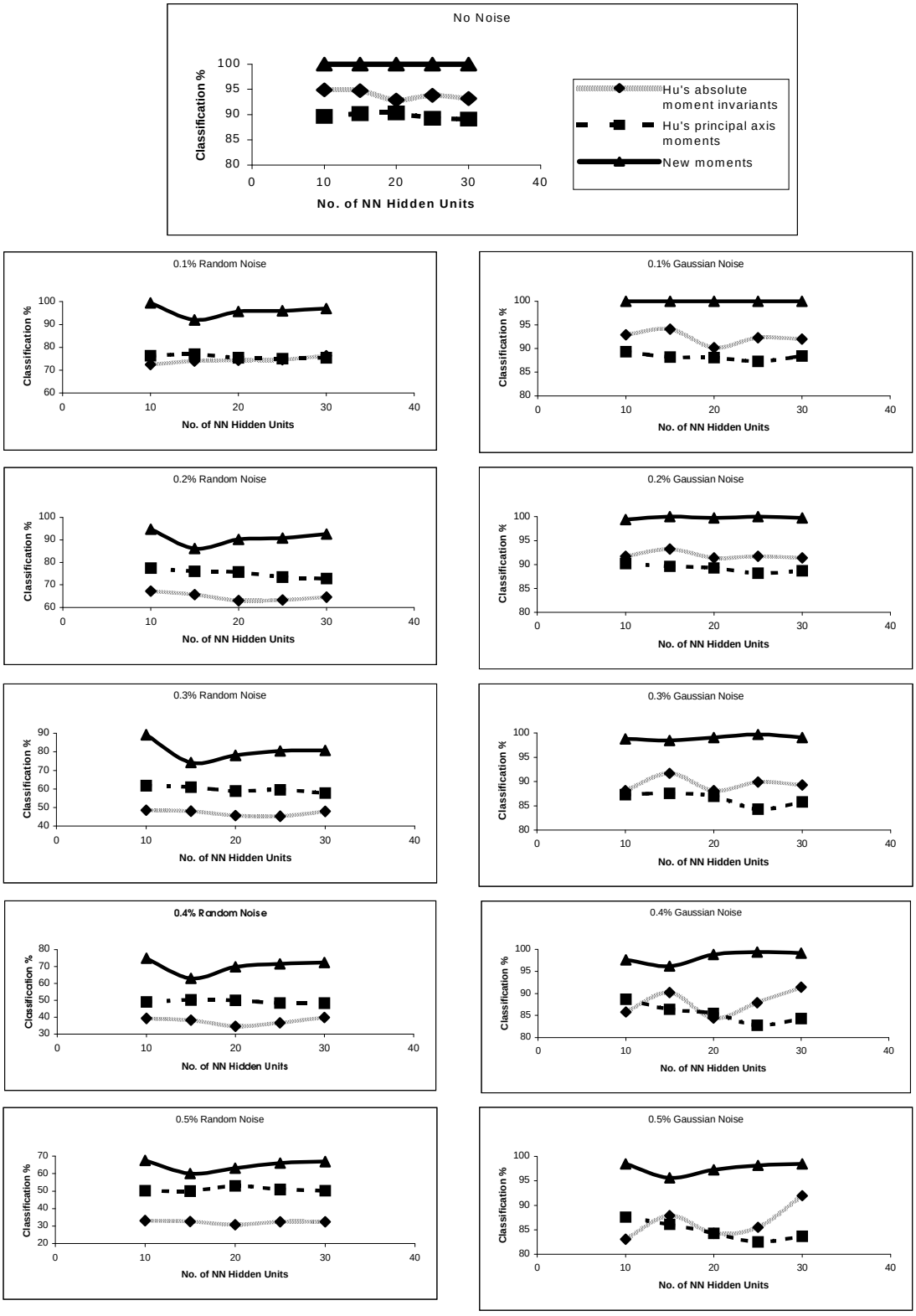

Figure 8: Results of NN classification for Gaussian and random type noisy images from Times New Roman font for both the Hu's moments and the new moments

References

[1] F.L. Alt, "Digital pattern recognition by moments", Journal of the Assn. for Computing Machinery, Vol. 9, No. 2, 1962, pp.240-258.

[2] R. Bamieh and R.J.P deFigueiredo, "A general moment attributed graph method for three dimensional object recognition from a single image", IEEE Transactions on Robotics and Automation, Vol. 2, No. 1, 1986, pp. 31-41.

[3] S.O. Belkasim, M. Shridhar and M. Ahmadi, "Pattern recognition with moment invariants: A comparative study and new results", Journal of the Pattern Recognition Society, Vol. 24, No. 12, 1991, pp. 1117-1138.

[4] H. Dirilten, "Pattern matching under affine transformations", IEEE Trans. on Computers, Vol. 26, No. 3, 1977, pp. 314-317.

[5] A. Dudani, K. J. Breeding, and R.B. McGhee, "Aircraft identification by moment invariant", IEEE Transactions on Computers C-26:39-45, 1977.

[6] E.B. Elliot, Algebra of Quantics, Oxford University Press, New York, 2nd edition, 1913.

[7] M. Gruber and K.Y. Hsu, "Moment-Based Image Normalization with High Noise Tolerance", IEEE Trans. on Pattern Analysis and Machine Intelligence, Vol. 19, No. 2, pp.136-139, Feb. 1997.

[8] Y.N. Hsu, H.H. Arsenault and G. April, "Rotational invariant digital pattern recognition using circular harmonic expansion", Applied Optics,Vol. 21, pp. 4012-4015, 1982.

[9] M.K. Hu, "Visual pattern recognition by moment invariants", IRE Trans. Information Theory, Vol. IT-8, pp. 179-187, February 1962.

[10] A. Khotanzad and J. H. Lu, "Classification of invariant image representations using a neural network", IEEE Trans. on Acoustics, Speech, and Signal Processing, Vol.38, pp.1028-1038, 1990.

[11] S. X. Liao and M. Pawlak, "On Image Analysis by Moments", IEEE Trans. on Pattern Analysis and Machine Intelligence, Vol. 18, No.3, pp. 254-266, March 1996.

[12] R. Palaniappan, Regular Moment Analysis for Pattern Recognition, Master thesis, University of Malaya, Malaysia, 1999.

[13] R. Paramesran, P.Ramaswamy and S. Omatu, "Regular Moments for Symmetric images", IEE Electronics Letter, Vol. 34, pp.1481-1482, July 1998.

[14] M. Pawlak, "On the Reconstruction Aspects of Moment Descriptors", IRE Trans. Information Theory, Vol. 38, No.6, pp. 1698-1708, November 1992.

[15] P. Raveendran, S. Jegannathan, and S. Omatu, "Classification of elongated and contracted images using new regular moments", IEEE World Congress on Computational Intelligence, Florida, U.S.A, Vol. 6, pp. 4154-4158, June 26-July 2, 1994.

[16] P.Raveendran and S.Omatu, "Neuro-pattern classification of elongated and contracted images", Information Sciences: Applications, U.S.A, Vol. 3, No. 3, pp. 209-221, May, 1995.

[17] S. Reddi, “Radial and angular moment invariants for image identification”, IEEE Trans. on Pattern and Machine Intelligence, 3:240-242 (1986).

[18] T.H.Reiss, “The Revised Fundamental Theorem of Moment Invariants”, IEEE Trans. on Pattern Analysis and Machine Intelligence, Vol. 13, No. 8, pp. 830-834, August 1991.

[19] A.P. Revees, R.J. Prokop, S.E. Andrews and F. Kuhl, “Three-dimensional shape analysis using moments and Fourier descriptors”, IEEE Trans. Pattern Analysis and Machine Intelligence, Vol. 10, pp. 937-943, November 1988.

[20] D.E. Rumelhart and J.L. McCelland, Parallel Distributed Processing: Exploration in the Microstructure of Cognition, MIT Press, Cambridge, MA, Vol. 1, 1986.

[21] Smith F.W. and Wright M.H., ”Automatic ship photo interpretation by the method of moments”, IEEE Transactions on Computers, Vol. 20, No. 9, 1971, pp. 1089-1095.

[22] M.R. Teague, “Image analysis via general theory of moments”, Journal of Optical Society of America, Vol. 70, pp. 920-930, August 1980.

[23] C.H. Teh and R.T. Chin, “On Image Analysis by the Method of Moments”, IEEE Trans. on Pattern Analysis and Machine Intelligence, Vol. 10, No. 4, pp. 496-513, July 1988.

[24] R.Y. Wong and E.L. Hall, ”Scene matching with moment invariants”, Computer Vision Graphics and Image Processing, Vol. 8, No.1, 1978, pp.16-24.